

## Investigation of Squirrel-Cage Induction Motor Properties

A. Degutis, P. Kostrauskas

Department of Electric Power Systems, Kaunas University of Technology,  
Studentų st. 48, LT-51367 Kaunas, Lithuania, phone: +370 37 351318; e-mail: algirdas.degutis@ktu.lt

### Introduction

Squirrel-cage induction machines dominate recently in miscellaneous electrical drives. This situation is determined by high reliability of this kind of electrical machines and also by simplicity of production technology of their rotors having aluminium windings. The appliance ranges of these machines widened substantially when frequency converters have been started to be used for the control of their rotation. It is necessary to mention at the same time that the squirrel-cage rotor casted by aluminium is more complicated from the theoretical point of view than wound-rotor – the winding of squirrel-cage rotor is poorly isolated from the core of electrical steel sheets. As shown in Fig. 1, the quadrature-axis currents  $I_q$ , producing additional losses, are created in the rotor [3]. The theory of squirrel-cage induction machine having rotor with aluminium winding is simplified by identifying the short circuited winding of rotor with the artificial one [1] which at first sight differs little from the real winding.

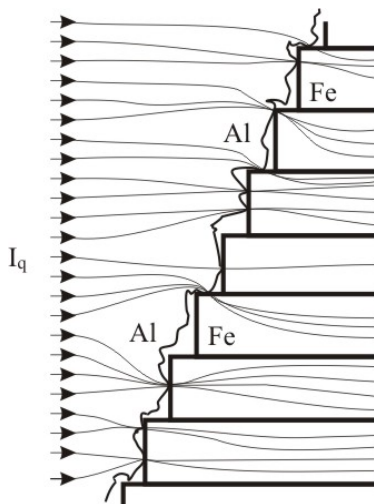


Fig. 1. Quadrature-axis currents in a squirrel-cage rotor of induction machine

The analysis of magnetic field of short circuited rotor's winding and results of experimental investigation are presented in the paper.

### Magnetic field of rotor

It is assumed in the investigation of rotor magnetic field that the rotor winding is polyphase and the polyphase current flows in the bars of rotor [1, 2, 5]. Such analysis of rotor magnetic field causes difficulties in the evaluation of geometrical parameters of rotor winding and in the determination of the location of winding bars in rotor slots. For example, in the monograph [1] the short circuited winding of rotor is being identified with the two-layer winding (Fig. 2).

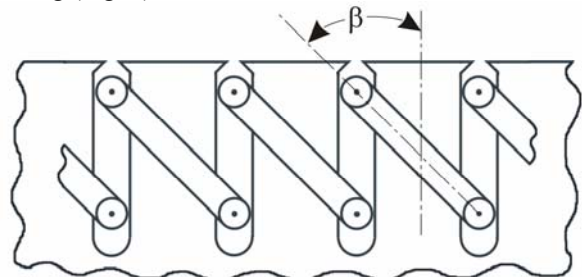


Fig. 2. Two-layer winding of induction machine's rotor

Using the expression of magnetic field's strength in the air gap of induction machine [1], we have

$$H_m(\alpha, t) = \frac{\sqrt{2}IN}{\pi\delta} \sum_{v=1}^{\infty} \frac{1}{v} \sin v \frac{\alpha_y}{2} \frac{\sin Nv \frac{\alpha_1}{2}}{N \sin v \frac{\alpha_1}{2}} \times$$

$$\times \left\{ \frac{\sin(v+1)\pi}{\sin\left[\frac{(v+1)}{m}\pi\right]} \sin\left[(\omega t + v\alpha) - \frac{m-1}{2}(v+1)\frac{2\pi}{m}\right] + \right.$$

$$\left. + \frac{\sin(v-1)\pi}{\sin\left[\frac{(v-1)}{m}\pi\right]} \sin\left[(\omega t - v\alpha) + \frac{m-1}{2}(v-1)\frac{2\pi}{m}\right] \right\}; \quad (1)$$

where  $N$  – number of coil's turns;  $I$  – effective value of current;  $\delta$  – length of air gap;  $v$  – order of space harmonic;  $\alpha_y$  – coil pitch;  $\alpha_1$  – angle between the coil

symmetry axes;  $\alpha$  – variable angle;  $m$  – number of winding's phases.

By using the formula (1) for the short-circuited rotor's winding (Fig. 2) in the case when the excitation field is single-phase, we receive

$$H_m^{(1)}(\alpha, t) = \frac{2\sqrt{2}IN}{\pi\delta} \sum_{v=1}^{\infty} \frac{1}{v} \sin v \frac{\alpha_y}{2} \frac{\sin Nv \frac{\alpha_1}{2}}{N \sin v \frac{\alpha_1}{2}} \times \cos v\alpha \sin \omega t. \quad (2)$$

The latter equation of magnetic field strength, written for the short-circuited rotor, does not take into account the geometrical peculiarities of two-layer winding of short-circuited rotor – for example, the angle  $\beta$  (Fig. 2).

There is shown in the paper that the strength of the rotor magnetic field  $H_m(\alpha, t)$  is under the influence of the angle  $\beta$ . The stator poles creating alternating magnetic field, and rotor magnetic core made of electrical steel sheets, on which the short-circuited turn 1-1 is placed and which freely rotates around its axis, are shown in Fig. 3.

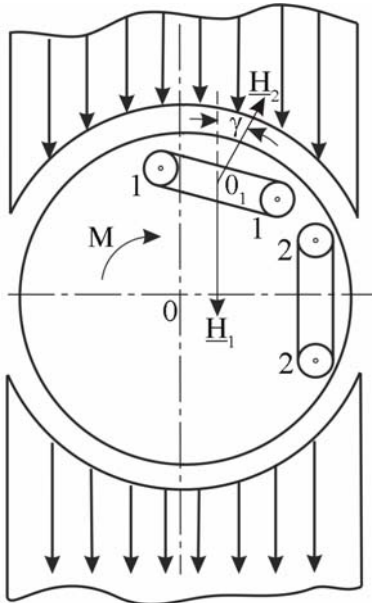


Fig. 3. Short-circuited turns on a rotor in the pulsating magnetic field of stator

The reluctance of the turn 1-1 to the magnetic field of stator [5] is

$$\underline{Z}_{\mu} = j \frac{2\pi f w^2}{\underline{Z}}; \quad (3)$$

where  $\underline{Z} = r + jx$  – electrical complex impedance of turn;  $w = 1$  – winding's number of turns;  $f$  – frequency;  $j$  – imaginary unit.

It is evident that

$$|\underline{Z}_{\mu}| > 0. \quad (4)$$

Therefore the increased reluctance in the area of the turn 1-1 may be treated as an increased air-gap. Consequently, the salient-pole rotor is available which is under the action of the reactive torque  $M$  this long until the turn 1-1 takes the position 2-2 (Fig. 3).

It is possible to conceive the origination of the torque  $M$  by invoking the laws of electrodynamics. Marking by  $\underline{H}_1$  the strength of stator magnetic field in the point  $O_1$ , and by  $\underline{H}_2$  – the strength of magnetic field of turn reaction, it is possible to notice that the  $\underline{H}_2$  lags in time from the  $\underline{H}_1$ . Hence, the strength of magnetic field  $\underline{H}_1$  rotates in the air-gap of induction motor to the counterclockwise direction, towards the strength of magnetic field  $\underline{H}_2$  (rotation angle  $180^\circ - \gamma$ ). This rotating magnetic field turns the poles of stator with the torque  $M$  to the counterclockwise direction. The rotor is turned with the same torque  $M$  to the clockwise direction because the stator is fixed to the foundation.

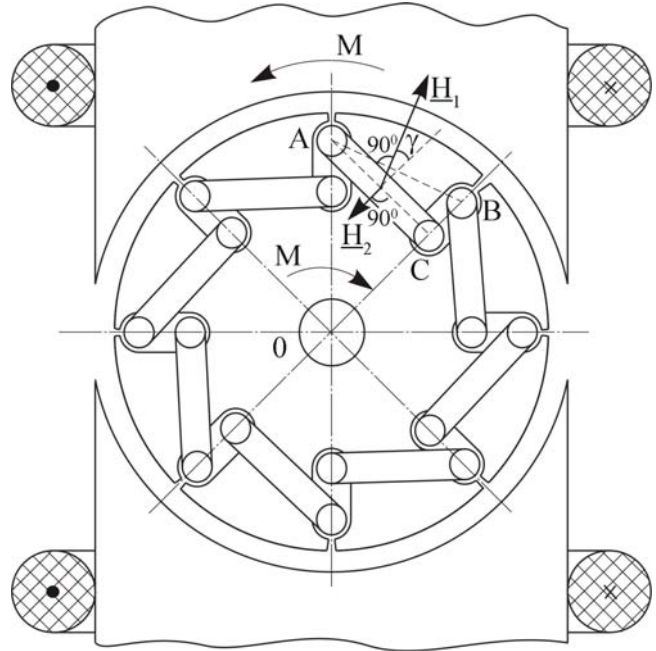


Fig. 4. Fragment of single-phase induction motor having the modified short-circuited rotor

In the Fig. 4 is shown the fragment of single-phase induction motor, having the rotor with the winding, made from short-circuited turns A-C, the angle  $\gamma$  of which is formed between its magnetic axis and the strength of magnetic field  $\underline{H}_1$  created by the stator winding. The element A-B (Fig. 4) of short-circuited rotor ring of traditional induction machines form the right-angle with the strength of magnetic field  $\underline{H}_1$ , and the angle  $\gamma = 0$ .

The pulsating magnetic field is created in the air-gap of single-phase induction motor when its stator winding is fed by alternating current and no current flows in the short-circuited turns of the rotor:

$$b(t, x) = \sum_{v=1}^{\infty} B_v \sin v \frac{\pi}{\tau} x \sin \omega t; \quad (5)$$

where  $b(t, x)$  – magnetic flux density depending on time and space.

The rotor tooth of the sector ABO (Fig. 4) is cut by magnetic flux  $\underline{\Phi}_1$ , which induces the electromotive force  $\underline{E}_2$  in the short-circuited turn A-C, shown in the Fig. 5, where  $\underline{I}_2$  – secondary current by reference to the primary winding flowing in the short-circuited winding of rotor; the current creates the magnetomotive force  $\underline{E}_2$  and the

magnetic flux  $\underline{\Phi}_2$ . Assume that the magnetic losses are vanishing. The time phases of magnetomotive force and of corresponding magnetic flux coincide in this case.

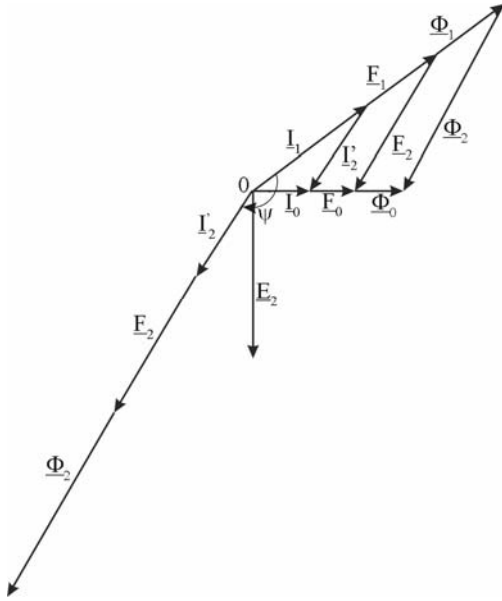


**Fig. 5.** The phasor diagram of electromagnetic values of the induction motor

It is possible to calculate the stator's magnetomotive force and the magnetic flux  $\underline{\Phi}_1$  when the magnetomotive force  $\underline{E}_0$ , the magnetic flux in the air-gap  $\underline{\Phi}_0$ , and the same values of short-circuited turn – the magnetomotive force  $\underline{E}_2$  and the magnetic flux  $\underline{\Phi}_2$  are available:

$$\underline{\Phi}_1 = \underline{\Phi}_0 - \underline{\Phi}_2. \quad (6)$$

The short-circuited turn A–C creates the magnetic flux  $\underline{\Phi}_2$  which lags in time from the magnetic flux  $\underline{\Phi}_1$  by angle  $\psi$  (Fig. 5).

### Torque of the induction motor

The magnetic fluxes  $\underline{\Phi}_1$  and  $\underline{\Phi}_2$  meet the following condition in space:

$$\left( \underline{\Phi}_1, \underline{\Phi}_2 \right) = \gamma. \quad (7)$$

Thus, the magnetic fluxes of rotor  $\underline{\Phi}_1$  and  $\underline{\Phi}_2$  create the electromagnetic torque [5]:

$$M_i = C \Phi_{1i} \Phi_{2i} \sin \gamma \sin \psi; \quad (8)$$

where  $C$  – constant;  $i$  – number of rotor's tooth.

This electromagnetic torque turns the stator to the counterclockwise direction and, because the stator of the induction motor does not move, therefore the torque turns the rotor to the clockwise direction.

By summing the torques created by all teeth of the rotor, we receive

$$M = \sum_{i=1}^{N_2} M_i = \sum_{i=1}^{N_2} C \Phi_{1i} \Phi_{2i} \sin \gamma \sin \psi; \quad (9)$$

where  $N_2$  – the total number of rotor's teeth.

Assume now that all short-circuited turns of the rotor are identical in the sense of their electromagnetic and geometric properties and therefore

$$\gamma = \text{const}, \psi = \text{const}. \quad (10)$$

The two-layer winding is often used for the wound-rotor of induction machines. Therefore the angle of magnetic axis of rotor winding section  $\gamma \neq 0$  (Fig. 4). However the initial starting torque  $M(9)$  is relatively small in this case because the angle  $\gamma$  amounts just  $3^\circ \div 5^\circ$ . Meanwhile the angle  $\gamma$  of the construction of the squirrel-cage rotor offered in this paper reaches  $25^\circ \div 35^\circ$ .

### Experimental part

The stator of conventional capacitor motor [7], the rated output power of which  $P_{2N} = 60$  W, is used in the experimental induction motor. The parameters of stator of the experimental induction motor are the following: the diameter of internal cylinder circle  $d_1 = 44 \cdot 10^{-3}$  m; the length of iron-core  $l_1 = 40 \cdot 10^{-3}$  m; the number of slots  $z_1 = 24$ . The sinusoidal two-pole single-phase winding made from 12 sections, is located in the stator of the motor. The short-circuited rotor was produced by engineer Petras Ukanis. The geometrical parameters of the rotor are the following: the diameter of outer cylinder  $d_2 = 43,6 \cdot 10^{-3}$  m; the length  $l_2 = 40 \cdot 10^{-3}$  m of iron-core made from electrical steel sheets, the thickness of which –  $0,5 \cdot 10^{-3}$  m; the diameter of rotor shaft  $d_3 = 10 \cdot 10^{-3}$  m; the number of slots  $z_2 = 17$ .

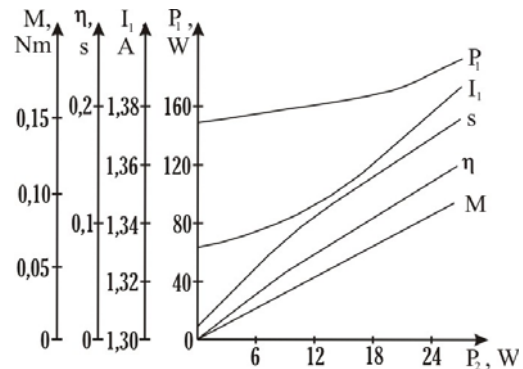


**Fig. 6.** Performance characteristics of the induction motor

The measured value of starting torque  $M_s = 0,031$  Nm. It is evident from the results of experiments that the single-phase induction motor with the squirrel-cage rotor having the construction described in the paper, creates the asynchronous torque, which is not discussed in a literature.

### Conclusions

The results of theoretical and experimental investigation confirm the proposition that the single-phase induction motor with the pulsating magnetic field of stator and with the squirrel-cage rotor having two-layer winding, develops the starting torque which is unequal to zero, on the contrary to what is claimed in the literature [1, 2, 5]. This electromagnetic effect also exists in the induction motors with the wound-rotor having the two-layer winding.

## References

1. **Heller B., Hamata V.** Harmonic Field Effects in Induction Machines. – Prague: Academy of Sciences, 1977. – 352 p.
2. **Binns K.J., Schmid E.** Some Concepts Involved in the Analysis of the Magnetic Field in Cage Induction Machines // Proc. IEE. – 1975. – P. 169 – 175.
3. **Schrub N.** Der Übergangswiderstand zwischen Blechpaket und Stäben gegossener Käfiglaufern // Elektrie. – 1980. – Bd. 29, Heft 6. – S. 316 – 319.
4. **Kostrauskas P.** Analysis of Electromagnetic Field in the Air Gap of Electrical Motors // Electronics and Electrical Engineering. – Kaunas: Technologija, 2003. – No. 1(43). – P. 32 – 36.
5. **Шафль М.** Электродинамические задачи в электрических машинах и трансформаторах. – Москва: Энергия, 1966. – 200 с.
6. **Костраускас П.** Однофазные явнополюсные асинхронные двигатели. – Каунас: Технология, 1995. – 124 с.
7. **Лопухина Е. М., Семенчуков Г. А.** Автоматизированное проектирование электрических машин малой мощности. – Москва: Высшая школа, 2002. – 511 с.

Submitted for publication 2007 02 28

### **A. Degutis, P. Kostrauskas. Investigation of Squirrel-Cage Induction Motor Properties // Electronics and Electrical Engineering. – Kaunas: Technologija, 2007. – No. 4(76). – P. 67–70.**

The assumption is often made when investigating induction motor's magnetic field that the rotor winding is polyphase and the polyphase current flows in the bars of rotor. The assumption causes difficulties in the evaluation of rotor winding's geometrical parameters and in the determination of bars location in the slots of the rotor. The geometrical peculiarities of squirrel-cage rotors winding, such as the angle  $\beta$ , are not taken into consideration by the theory of squirrel-cage induction machine given in literature. It is proved that the strength of magnetic field, creating the torque rotating the rotor, depends on the angle  $\beta$ . The expression of resultant torque created by squirrel-cage rotor's teeth of induction motor has been derived. The two-layer winding of rotor is often used for the wound-rotor induction machines. In this case the angle of rotor winding section's magnetic axis  $\gamma \neq 0$ . Though the initial starting torque of induction motor having wound-rotor with two-layer winding is relatively small because the angle  $\gamma$  amounts just  $3^\circ - 5^\circ$ . Meanwhile the angle  $\gamma$  of squirrel-cage rotor's construction referred in the paper reaches  $25^\circ - 35^\circ$  and therefore the induction motor having the squirrel-cage rotor of described construction creates relatively larger initial starting torque. Ill. 6, bibl. 7 (in English; summaries in English, Russian and Lithuanian).

### **A. Дегутис, П. Костраускас. Исследование свойств асинхронного двигателя с короткозамкнутым ротором // Электроника и электротехника. – Каунас: Технология, 2007. – № 4(76). – С. 67–70.**

При исследовании магнитного поля ротора асинхронного двигателя предполагается, что роторная обмотка является многофазной, а по стержням ротора протекает многофазный ток. Таким допущением осложняется оценка геометрических параметров роторной обмотки и размещения стержней обмотки в пазах ротора. Представляемая в литературе теория асинхронной машины не учитывает геометрических особенностей короткозамкнутой обмотки ротора, например, угла  $\beta$ . Доказано, что напряжённость магнитного поля ротора, создающая момент, вращающий ротор, зависит от угла  $\beta$ . Выведено выражение суммарного вращающего момента, создаваемого зубцами короткозамкнутого ротора асинхронного двигателя. В случае асинхронного двигателя с фазным ротором, имеющим двухслойную обмотку, угол магнитной оси секции роторной обмотки  $\gamma \neq 0$ . Но такой асинхронной двигатель создаёт относительно малый начальный пусковой момент, поскольку угол  $\gamma$  достигает лишь  $3^\circ - 5^\circ$ . Угол  $\gamma$  короткозамкнутого ротора, конструкция которого предложена в этой работе, достигает  $25^\circ - 35^\circ$  и поэтому такой асинхронный двигатель развивает относительно большой начальный пусковой момент. Ил. 6, библи. 7 (на английском языке; рефераты на английском, русском и литовском яз.).

### **A. Degutis, P. Kostrauskas. Asinchroninio variklio su narveliniu rotoriumi savybių tyrimas // Elektronika ir elektrotechnika. – Kaunas: Technologija, 2007. – Nr. 4(76). – P. 67–70.**

Tiriant asinchroninio variklio rotoriaus magnetinį lauką dažnai daroma prielaida, kad rotoriaus apvija daugiafazė, o rotoriaus stiebais teka daugiafazė srovė. Ši prielaida apsunkina rotoriaus apvijų geometrinių parametrų bei stiebų išsidėstymo grioveliuose įvertinimą. Literatūroje pateikiama asinchroninės mašinos su narveliniu rotoriumi teorija neįvertina narvelinio rotoriaus apvijų geometrinių ypatumų, pavyzdžiui, kampo  $\beta$ . Įrodyta, kad kampas  $\beta$  turi įtakos rotoriaus magnetinio lauko, kuriančio rotoriaus sukimo momentą, stipriui. Išvesta asinchroninio variklio narvelinio rotoriaus dantų kuriamo suminio sukamojo momento išraiška. Asinchroninių mašinų su faziniu rotoriumi rotoriaus apvija dažnai daroma dvisluoksniė. Šiuo atveju rotoriaus apvijų sekijos magnetinės ašies kampas  $\gamma \neq 0$ . Tačiau asinchroninio variklio, turinčio fazinį rotorių su dvisluoksne apvija, pradinis paleidimo momentas yra santykinai mažas, nes kampas  $\gamma$  tesiekia vos  $3^\circ - 5^\circ$ . Šiame darbe pateiktos narvelinio rotoriaus konstrukcijos kampas  $\gamma$  siekia  $25^\circ - 35^\circ$ , todėl asinchroninis variklis, turintis aprašytosios konstrukcijos narvelinį rotorių, kuria santykinai didelį pradinį paleidimo momentą. Il. 6, bibl. 7 (anglų kalba; santraukos anglų, rusų ir lietuvių k.).